Theor Chem Acc (2001) 106:137–145
DOI 10.1007/s002140100253

Theoretical
Chemistry Accounts

Regular article

Modelling radiation-induced damage in the *lac* operator–*lac* repressor complex. DNA damage: 8-oxoguanine

D. Sy[1,2], **C. Flouzat**[1,2], **S. Eon**[1], **M. Charlier**[1], **M. Spotheim-Maurizot**[1]

[1]Centre de Biophysique Moléculaire, CNRS, rue Charles-Sadron, 45071 Orléans Cedex 2, France
[2]Faculté des Sciences, B.P. 6759, Université d'Orléans, F-45067 Orléans Cedex 2, France

Received: 20 July 2000 / Accepted: 5 January 2001 / Published online: 3 April 2001

Abstract. Among the DNA lesions induced by ionising radiation, one of the most abundant base modifications is that of guanine (G) into 8-oxo-7-hydro-2′-deoxyguanosine (oxoG). The *Escherichia coli lac* operator–*lac* repressor complex bearing one or several oxoG was studied by molecular modelling. The initial structure of the complex was obtained from the Protein Data Bank (1CJG entry – model 1). Systematic replacements of G by oxoG were carried out. Modelling involved energy-minimisation and simulated-annealing techniques using the Amber force field. Depending on its location along the DNA sequence, oxoG induces modifications of the energetic characteristics of the complex, the electrostatic potential distribution on the surfaces of the DNA and of the protein, the DNA and protein conformations and DNA and protein flexibility. In the case of the replacement of G by oxoG at position 8 of the fragment, the most noticeable effects are a 13% decrease in the interaction energy and a 14% reduction in the number of intermolecular hydrogen bonds, all other effects being much weaker. Therefore, we may conclude that the presence of one or several such base modifications is insufficient to account, alone, for the experimental observation of the radiation-induced decrease of *lac* operator–*lac* repressor binding extent.

Key words: Ionising radiation – Oxoguanine – DNA–protein complex – Molecular modelling

1 Introduction

Ionising radiation induces DNA damage, such as strand breaks, sugar lesions, abasic sites and base modifications [1]. These damages are mostly sparsely distributed along DNA in the case of low lineal energy transfer (LET) radiation, but the proportion of clustered lesions increases with increasing LET [2, 3]. Mutagenesis, carcinogenesis and apoptosis are some biological consequences of these damages [4]. The dysfunction of DNA–protein systems regulating replication and gene expression may be one of the causes of such effects.

One of the most abundant radiation-induced or endogenous oxidation-induced base modifications is that of guanine (G) into 8-oxo-7-hydro-2′-deoxyguanine (oxoG), which seems to be involved in both mutagenesis and carcinogenesis [5, 6]. The presence of this damage at some positions of the cognate target DNA sequence decreases the binding of a sequence-specific binding protein, the transcription factors Sp1. The decrease varies from 0 to 28% as a function of the position at which the lesion was introduced [7]. The reduced protein binding affinity can be due to DNA structural or flexibility changes. Until now no global structural changes but only some differences in thermal and thermodynamic properties [8, 9] and subtle changes to DNA dynamics were evidenced for short oligomers containing one oxoG [10].

The *Escherichia coli* lactose operon is one of the most studied and best understood systems of gene expression and regulation. The *lac* repressor is a tetrameric protein constituted by a tetrameric core and four headpieces. It binds tightly to the *lac* operator, a DNA region of a specific sequence, preventing the expression of the structural genes of the *lac* operon [11]. The protein–DNA interaction occurs via the binding of two headpieces to the operator. Each headpiece is formed by three α helices (H1–H3), two of them (H1 and H2) constituting a helix-turn-helix (HTH) motif responsible for the specific interaction with the operator. H2 is called the recognition helix. The headpiece is connected to the core by a hinge region that adopts a helical conformation (H4) only when the repressor binds to the operator. The tightest binding operator is the symmetrical operator SymL(-1), a palindrome of the left half of the wild-type operator, lacking the central base pair. This operator, which differs from the wild-type one by two nucleotides, was used for structural studies of the *lac* operator–*lac* repressor complex. The structure of a complex formed by one tetrameric *lac* repressor with two engineered SymL(-1) operators was solved by X-ray

Correspondence to: D. Sy
Contribution to the Symposium Proceedings of Computational Biophysics 2000

crystallography [12]. According to it, the HTH motif fits into the major groove, whereas the H4 hinge helix interacts with the minor groove of DNA. To accommodate H4 into the minor groove, the DNA is distorted (widening of the minor groove, etc.) and bends away from the repressor. The distortion and the bent are localised at the centre of the operator.

Recently, the structure of the complex formed in solution by one SymL(-1) operator and two repressor headpieces, each containing the four α helices, was solved by nuclear magnetic resonance (NMR) spectroscopy and restrained molecular dynamics [13]. This structure is globally quite similar to the crystallographic structure.

Upon γ-ray irradiation of a solution containing the *lac* operator–*lac* repressor complex a decrease in the amount of the DNA–protein complex and, thus, an increase in the amount of free DNA were observed by retardation gel electrophoresis. To assess which DNA or protein damage is responsible for the effect observed, an important number of experiments using oligonucleotides and peptides bearing only one type of damage would be necessary (for an example, see Ref. [7]). To reduce the number of synthesised modified oligonucleotides and peptides, a systematic screening of the effects of different types of DNA and protein lesions by molecular modelling might be helpful. We present here an example of such a molecular modelling study in which the studied lesion is the abundant modified base, 8-oxoguanine (8-oxoG).

In the molecular modelling study we searched the modifications induced in this complex by the introduction of one or more oxoG into DNA. Unique lesions model the sparse damage induced by low LET radiation, whereas multiple lesions model the clustered damages induced by high LET radiation. OxoG was introduced at different positions in order to investigate sequence-dependent effects. The initial structure of the complex was obtained from the Protein Data Bank (PDB) databank (1CJG entry – model 1 [13]).

Molecular mechanic energy-minimisation techniques were applied to evidence possible oxoG-induced local conformational changes on both partners. Moreover, the consequences on the global structure and energy were analysed. Since it is critical for the complexation, the electrostatic potential distributions at the surface of DNA and of the protein in the modified complex were compared to those in the intact complex.

Modifications of DNA bending and flexibility seem to affect protein binding, as suggested in the case of the TATA-box DNA target of the protein TBP; therefore, the domains of high flexibility were determined by a simulated annealing method.

The results are discussed in connection with our recent experimental data showing a radiation-induced splitting of the complex.

2 Materials and methods

The starting structure for the *lac* operator–*lac* repressor complex studied was the first model of the NMR structure from the PDB with the code 1CJG [13], comprising two headpieces and one operator. It encompasses

1. Two repressor headpieces, thus two symmetrical 62 amino acid chains, A and B:
   M-K-P-V-T-L-Y-D-V-A_{10}-E-Y-A-G-V-S-Y-Q-T-V_{20}-S-R-V-V-N-Q-A-S-H-V_{30}-S-A-K-T-R-E-K-V-E-A_{40}-A-M-A-E-I-N-Y-I-P-N_{50}-R-V-A-Q-Q-L-A-G-K-Q_{60}-S-L
   The elements of the secondary structure of each chain are helix H1 (L_6-A_{13}), helix H2 (Y_{17}-V_{24}), helix H3 (A_{32}-L_{45}), helix H4 (R_{51}-L_{56}) and the connecting loops.
2. One DNA operator, a duplex palindromic 22 base pair sequence:
   C strand: 5′-G_1-A-A-T-T -G_6-T-G_8-A-G_{10}-C-G_{12}-C-T-$\mathbf{C_{15}}$-A-C-A-A-T -T-C-3′
   D strand: 3′-C-T-T -A-A-C-A-C-T-C-G_{12}-C-G_{10}-A-$\mathbf{G_8}$-T-G_6-T-T-A-A-G_1-5′

Graphic representations and modelling computations were performed using an SGI R10000 workstation, using Tripos (St Louis, Mo) SYBYL software.

The only DNA damage considered in the present study was the base modification of G into 8-oxoG (O). The new nucleotide O was thus built and added to the standard DNA dictionary. Then, on the initial NMR structure, the G/O replacement either at one single site or at multiple sites was undertaken. The corresponding complexes are labelled according to the strand and position, *i*, of the O nucleotide i.e. C/O*i* (single damage) or D/O*i*, O*j* (multiple damage).

All energy calculations were carried out with an implicit aqueous environment, i.e. with a linear distance-dependent dielectric constant. The following specifications were used: Kollman charges, Amber force field, 12-Å cutoff distance, Powell minimisation method with a 10^{-3} energy gradient termination option. At first, in the molecular mechanics comparative study, each complex was energy-minimised using the previously described specifications.

For the unmodified complexed DNA, the atom accessibility to a sphere of the size of an OH· radical (1.2 Å) was calculated with the SAVOL algorithm included in SYBYL.

In order to enlarge the conformational space exploration, and to determine the secondary structure elements of greater stability, a simulated annealing protocol, with a 1ps-heating phase up to 500 K and an exponential 2-ps annealing phase down to 250 K, was used on half complexes, the other ones being fixed. During the simulation torsional and distance range constraints were applied. They concern, respectively, the backbone of the four protein helices and the terminal base pair (Watson–Crick partner atoms). The structures obtained at the end of each cycle were minimised further.

The potentials on the electron density surfaces were calculated and represented using the SYBYL MOLCAD module. DNA structural analysis was undertaken via CURVES [14]. The abscissa numbering in the representation of helicoidal parameters refers to the numbering of the C strand (the modification in D/O8 corresponds to the number 15, see bold characters in sequence above).

The total DNA curvature is calculated as the angle between the oriented segments connecting one terminal G–C pair centroid to the two central G–C central pairs centroid and the latter to the other terminal G–C pair centroid.

The minor groove width was measured according to Neidle's procedure [15]. The abscissa numbering in the representation of the minor groove width refers to scheme 1:

C strand ⇒

$G_1{=}A_2{=}A_3{=}T_4{=}T_5{=}G_6{=}T_7{=}G_8{=}A_9{=}G_{10}{=}C_{11}{=}G_{12}{=}C_{13}{=}T_{14}{=}C_{15}{=}A_{16}{=}C_{17}{=}A_{18}{=}A_{19}{=}T_{20}{=}T_{21}{=}C_{22}$

|2 |3 |4 |5 |6 |7 |8 |9 |10 |11 |12 |13 |14 |15 |16 |17 |18 |19 |20

$C_{22}{=}T_{21}{=}T_{20}{=}A_{19}{=}A_{18}{=}C_{17}{=}A_{16}{=}C_{15}{=}T_{14}{=}C_{13}{=}G_{12}{=}C_{11}{=}G_{10}{=}A_9{=}G_8{=}T_7{=}G_6{=}T_5{=}T_4{=}A_3{=}A_2{=}G_1$

D strand ⇐

Scheme 1. Numbering of the base-pairing used in the measurement of the minor groove width

The protein helix displacements relative to the DNA molecule were estimated by calculating for each helix the distance between the geometric centre of its backbone atoms and the closest DNA base pair centre.

3 Results and discussion

3.1 Background

The retardation gel electrophoresis of a mixture containing a sequence specific protein and radioactively labelled DNA fragments bearing the target sequence is able to separate the free DNA fragments from those bound to the protein. This technique was applied to a mixture of *E. coli lac* repressor proteins and of 36 bp DNA fragments bearing the 22 bp Sym L(-1) *lac* operator sequence. Conditions in which all fragments are complexed (large excess of protein) were used. In this case, each fragment is bound to two headpieces of one repressor, as in the NMR-based structure of the complex used in the calculations.

It was observed that the γ-ray irradiation of the solutions leads to a dose-dependent decrease in the amount of complexed DNA and, consequently, to an increase in the amount of free DNA. A dose of 240 Gy is necessary to decrease the amount of complex to 50% of its initial value. It was concluded that the irradiation disfavours the binding of the protein to DNA.

Modifications of the conformation and/or flexibility of the partners may be induced by the degradation of bases and sugars (DNA) and/or of amino acids (proteins). If they led to weaker DNA–protein interactions, these modifications could be at the origin of the destruction of the complex.

An experimental systematic screening of the consequences of each of the possible damages demands the synthesis of a huge number of molecules. Molecular modelling allows the *in silico* building of molecules bearing unique lesions at controlled positions of the sequences. The lesion studied here is the most abundant base modification, that of G into oxoG.

3.2 Single and multiple oxoG damage

OxoG is formed by the oxidation of the radical obtained after the addition of an $OH^{\cdot}$ radical to the C8 position of G; therefore, the accessibility of the C8 atom to an $OH^{\cdot}$ radical plays the major role in the radiation-induced production of oxoG. The accessibility to $OH^{\cdot}$ radicals of the C8 atom of all the G of the two strands C and D of the complexed DNA was measured. If one ignores G1 for end-effect reasons, the order of accessibilities is G8 (3.5 $Å^2$) > G10 (1.5 $Å^2$) > G12 (0.1 $Å^2$) > G6 (0 $Å^2$).

The minimised complexes bearing one or more oxoG at various positions present different energy values. Despite the system sequence symmetry, the effects of G/O replacements at the same position on the C or D strands are not equivalent (result not shown). This is probably due to the asymmetry of the PDB initial complex structure.

In the case of the D strand, the total energies together with the electrostatic and van der Waals energies are displayed in Fig. 1. For some replacements an increase of about 50 kcal/mol for the total energy is observed. The electrostatic and the van der Waals energies present similar changes. For other replacements no energy change is observed.

For the same replacements a decrease of about 1° of the total DNA curvature is observed (Fig. 1). In these cases, the corresponding straightening is accompanied by a 1-Å lengthening (from about 63.5 to 64.5 Å) of the DNA molecule. The following correlation is observed: the less stable complexes exhibit the lowest curvature and the longest total length.

From these profiles, roughly two types of behaviour can be discriminated: for some replacements, a decrease in the absolute value of the total energy of the complex, a decrease in the curvature and a lengthening of DNA, whereas for others there is no change in these characteristics.

These "switchlike" complex-destabilising and DNA-straightening effects depend on the replacement position along the sequence. For single replacements, the effect is zero for locations near the DNA centre and nonzero for

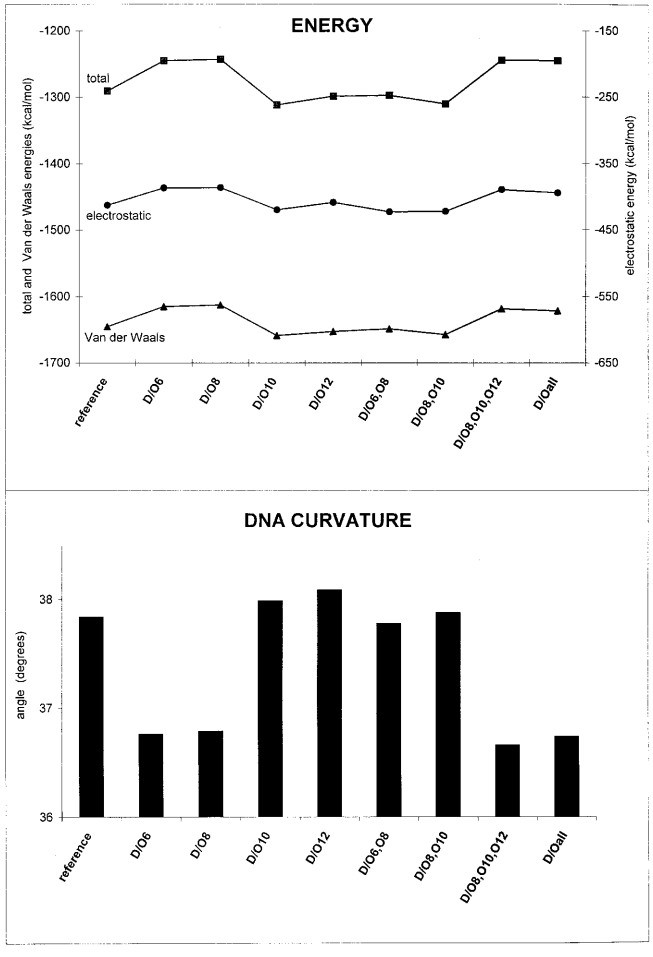

Fig. 1. Two global parameters for native and modified complexes. *Top:* total energy and its components: electrostatic and van der Waals energy. *Bottom:* global DNA curvature

eccentric locations. This effect originates in the relative protein/DNA positions: the H4 helix located in the GCGC minor groove contributes to the stiffening of this zone, whereas the H2 helix located in the GTGA major groove does not. Moreover, a sequence-dependent difference in the DNA stability may contribute to the effect: the GCGC central zone is probably intrinsically more stable than the flanking GTGA zones [16].

The effects of replacement at multiple sites also present "switchlike" behaviour. Moreover, these effects are never stronger than that of single ones. In some cases, combining replacements that, separately, lead to changes can result in a zero effect (e.g. D/O6, O8). In contrast, a combination of replacements that separately had no effect can lead to a nonzero effect (results not shown).

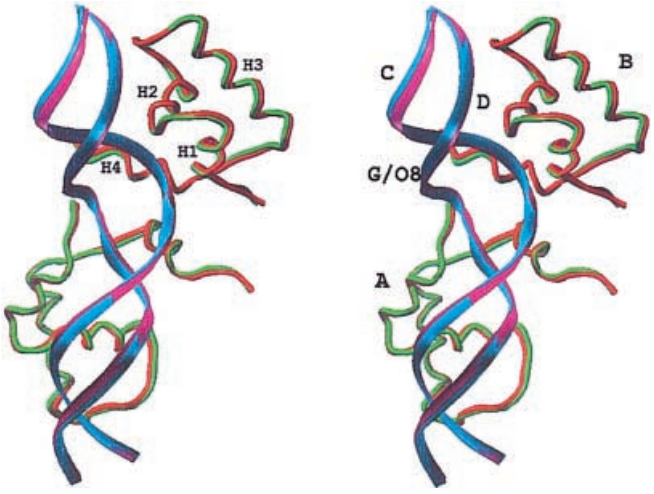

Fig. 2. Stereoview of the superposition of native and modified complexes. For the native D/G8 complex, the DNA skeleton is displayed as a magenta ribbon and the protein backbone as a *green tube*. For the modified D/O8 complex, the DNA skeleton is displayed as a *cyan ribbon* and the protein backbone as a *red tube*

For an extended analysis we compare in the following mainly the reference D/G8 complex with the D/O8 one (bearing a single oxoG instead of G at position 8 of the D strand) (Fig. 2). According to the accessibility of the radiolytic attack position (C8 of G) to $OH^{\cdot}$ radicals, D/G8 is the most likely to undergo a G→O modification. Moreover, the G8 base is involved in hydrogen-bonding interactions with Tyr17, the first amino acid of the repressor recognition helix H2.

3.3 DNA conformation

Besides the global curvature, the minor groove width undergoes some modifications upon G/O replacements. For various complexes with a single oxoG on the D strand, the profiles along the sequence are displayed in Fig. 3. On each side of the central GCGC area with a wide minor groove (about 16Å) corresponding to the binding site of the two repressor antiparallel H4 hinge helices, low values are observed. It is noteworthy that the G8/O8 replacement induces a profile modification not only at the replacement site (width increase) but that it also extends along the DNA sequence. Minor groove modifications are observed as far as 12 nucleotides away, thus beyond the GCGC central area.

Such long-distance effects are also observed on several DNA conformational parameters. The profiles of one axis, one interbase and one backbone parameter are displayed in Fig. 4. Sugar puckers undergo local changes from C2′-endo to C1′-exo and from C1′-exo to O1′-endo on nucleotides D/G6 and D/T7, respectively.

3.4 Protein conformation

In the case of the G8/O8 replacement, the secondary and tertiary structures of the protein are largely conserved. However, the repressor compactness is slightly reduced: the accessible surface of the core hydrophobic residues

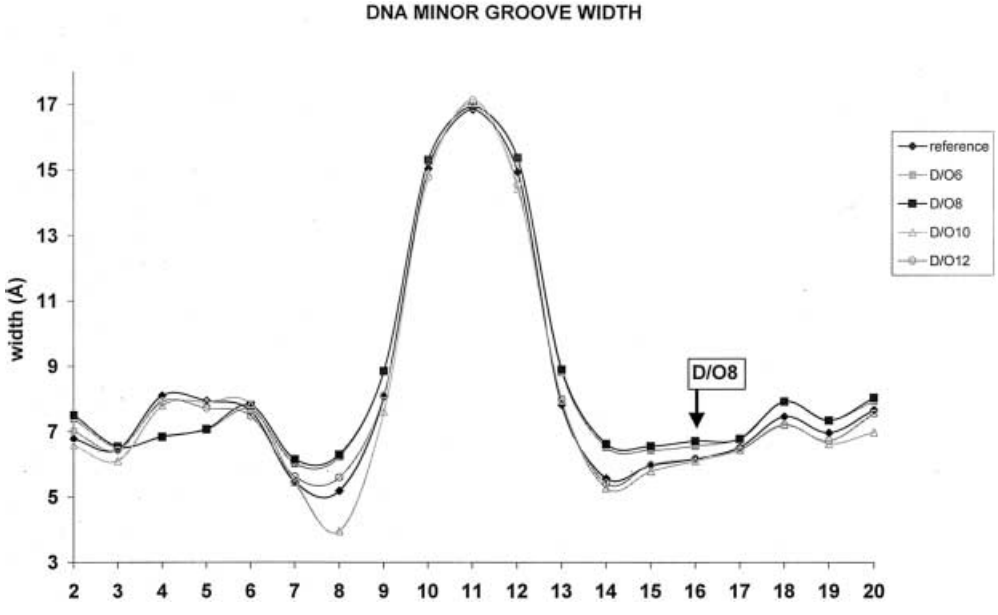

Fig. 3. DNA minor groove width for native and modified complexes. The *numbering* on the abscissa refers to base couples on opposite strands (cf. Sect. 2)

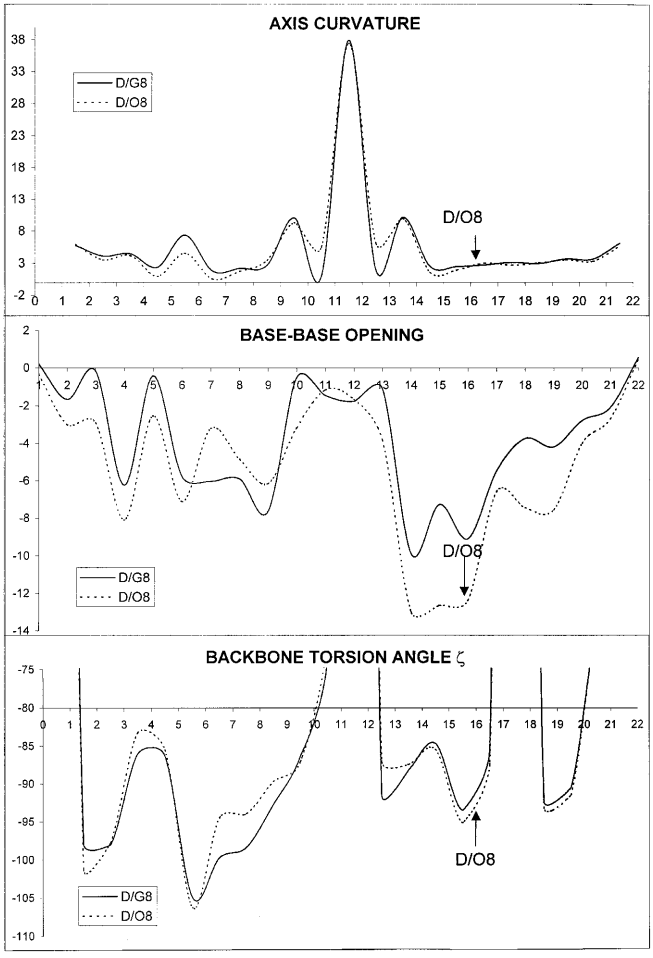

Fig. 4. DNA helical parameter profiles analysed with CURVES for the D/G8 native and D/O8 modified complexes. The numbering on the abscissa refers to the C strand 5′→3′ nucleotides (cf. Sect. 2). The *ordinates* correspond to the angles expressed in degrees

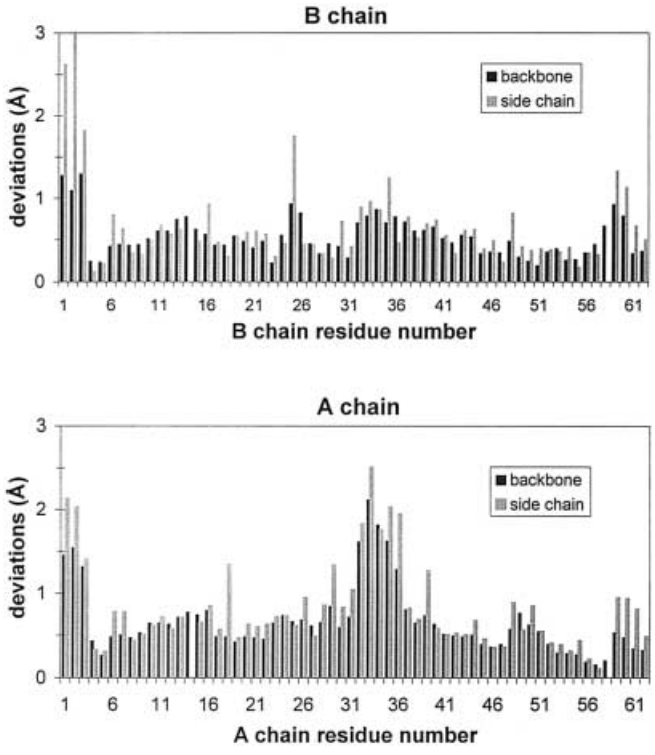

Fig. 5. Repressor heavy atoms deviations for the D/O8 relative to the D/G8 complex

undergoes a 2% increase. Moreover the H1–H4, H2–H3 and H2–H4 distances are slightly increased. The deviations between the structures of the two complexes are calculated on the backbone and the side-chain atoms of both protein chains, A and B. Interestingly, the histograms displayed in Fig. 5 show a larger effect on chain A, far from the G/O replacement site, than on chain B, closer to the site. The protein most affected areas correspond to the N and C terminals and to the 32–37 residues belonging to the H3 helix. This helix that ensures the headpiece cohesion is translated along its axis and is also rotated around its C terminal centroid so that the most displaced residues are the first ones on the N terminal.

3.5 Surface potentials

As the global electrostatic energy plays a key role in the interaction between the DNA and the protein we examine their surface potentials. The potentials on the surface of the DNA and the protein in the D/G8 and D/O8 complexes are represented in Fig. 6.

In the D/O8 complex the DNA surface potentials are less negative, thus less attractive for the positive potential zones of the protein involved in the recognition. The reduction in the attractive potential on the DNA moiety can be explained by a decrease in the charge density due to a weaker DNA curvature. The effect of the G/O replacement on the potentials is variable over the molecule surface in relation to the variations of the geometrical parameters.

In the D/O8 complex the potential on the surface of the protein is lower than in the D/G8 complex, especially in the zones closest to the DNA molecule; the electrostatic interaction of the protein with DNA is thus weakened. The analysis of the helix deviations (Fig. 5) and the structure examination evidences a translation of the H3 helix accompanying a slight protein decompaction. This effect results in a spacing of the positively charged protein residues participating in the DNA anchoring and consequently to the reduction of the electrostatic potential in the H2 and H4 interaction areas (Fig. 6).

3.6 Interactions

From the comparison between the D/G8 and D/O8 minimised complexes, several energetic and structural features of the interaction can be deduced (Table 1).

The oxoG damage at location G8 on the D strand results in a higher global energy and thus in the destabilisation of the complex. The energies of each partner are not significantly modified, but their interaction becomes energetically less favourable. This is

Table 1. DNA–protein interaction relative characteristics, upon G/O replacement, for the D/G8 native and the D/O8 modified complexes

	D/G_8	D/O_8	Relative difference
Complex total energy	−1292	−1246	−3.6%
DNA energy	−332	−337	1.5%
Protein energy	−571	−571	0%
Interaction energy ($kcalmol^{-1}$)	−389	−338	−13%
Intermolecular hydrogen bonds	36	31	−14%
H1 centre – (D/G_8–C/C_5) centre (Å)	17.2	18.1	5%
H2 centre – (D/T_7–C/A_{16}) centre (Å)	12.9	13.0	0.5%
H3 centre – (D/T_7–C/A_{16}) centre (Å)	21.6	22.0	2%
H4 centre – (D/C_{11}, G_{12}–C/G_{12}, C_{11}) centre (Å)	9.3	9.6	3%

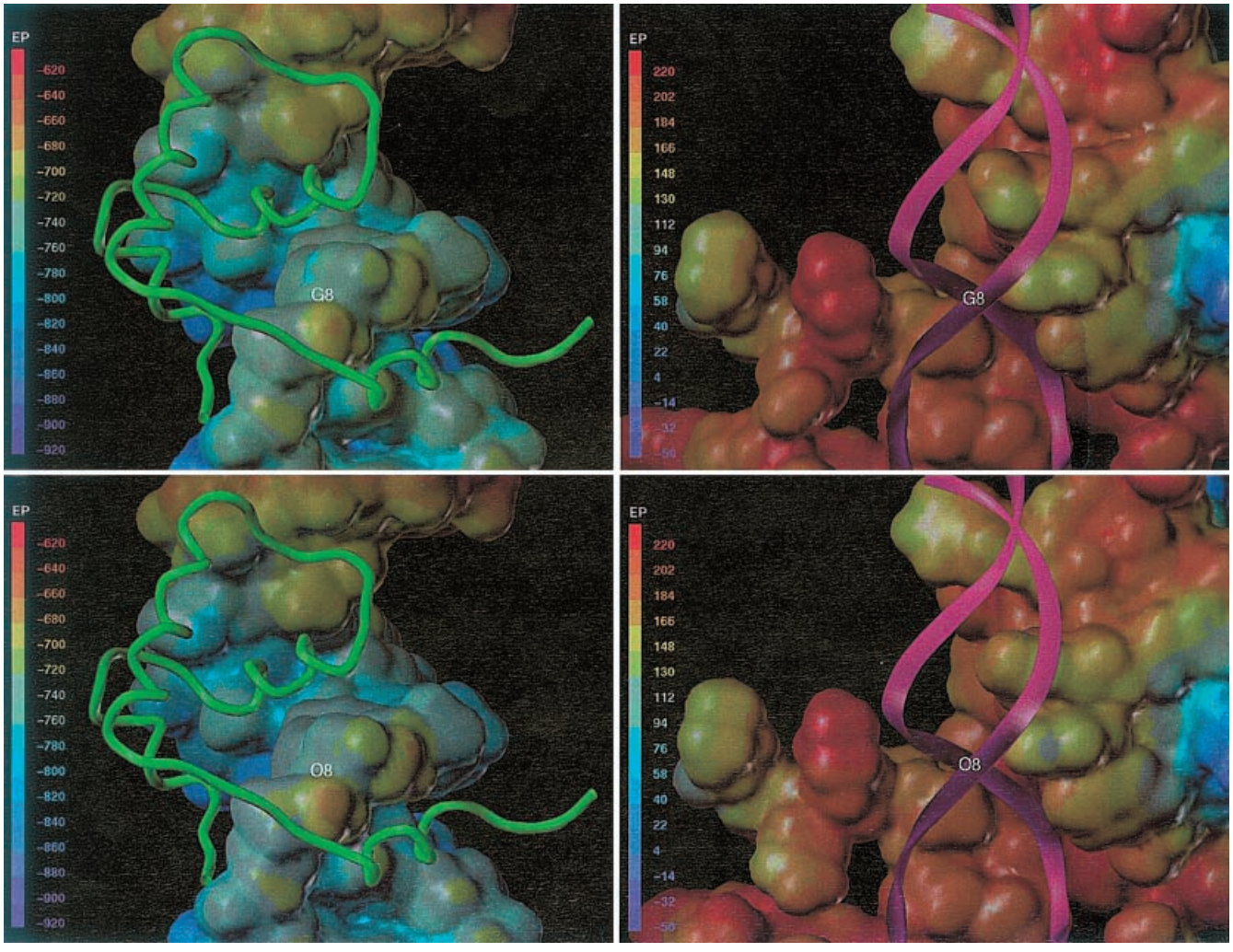

Fig. 6. Electron density surfaces colored by potential for native (*top views*) and modified complexes (*bottom views*). The *left* and *right views* are relative to the DNA and the protein respectively and they are rotated from 160° to each other in order to display their interface

mainly due to the weakening of the electrostatic and van der Waals interactions (Fig. 1) accompanied by a reduction in the number of intermolecular hydrogen bonds (Table 1).

The weakening of the electrostatic interactions was discussed in Sect. 3.5. The reduction in the van der Waals interaction results from looser operator–repressor contacts: all helices are more distant from DNA in the D/O8 than in the D/G8 complex (Table 1). It is noteworthy that the smallest relative deviation occurs for the H2 recognition helix. The order of deviations is H2 < H3 < H4 < H1.

Two types of intermolecular electrostatic interactions between DNA and the protein have to be distinguished: saline bridges or hydrogen bonds between the protein charged residues and the DNA phosphate groups (e.g. His29-T4), and hydrogen bonds between protein polar residues and the DNA bases (e.g. Tyr17-G8). The bonds

of the first category play a role in the anchoring of the headpieces to the DNA and these bonds are located on opposite ends of the protein partner. These bonds are quite conserved in the O8 complex. The explanation might lie in the flexibility of the long side chains of the residues involved in anchoring, which allows the relative adjustment of partners. The bonds of the second category are less stable: they look rather like a fine setting of the interaction and should be disrupted earlier than the saline bridges in a dynamic unbinding process. Indeed, the bonds that are disrupted owing to the G/O replacement belong to this category (e.g. Gln18-A16).

3.7 Simulated annealing

For each D/G8 and D/O8 complex, the backbones of five structures obtained from the simulated annealing procedure are superimposed in Fig. 7.

Globally the DNA skeleton is more disordered in the O8 complex than in the G8 one. This increased dispersion is the expression of increased molecular flexibility. In the O8 complex, the dispersion starts in the central zone, at D/C11: conformational modifications concern bases and the skeleton and get overamplified further in the sequence with the flipping out of the D/G10 and C/C15 and C/A16 bases. For the reference G8 complex the dispersion starts two bases further at the D/A9 base level, and the progressive base tilt and opening do not appear so drastic.

Conversely, the protein B-chain backbones are globally less disordered in the O8 complex, except for the H4 hinge helix. The dispersion measured on the C_α atoms of the H4 helix reaches an average value of 4.6 Å (against 0.6 Å in the reference complex) and corresponds to a lateral displacement relative to the DNA. This dispersion is driven by the previously described DNA large flexibility in the H4 binding site. On the other hand, the H2 recognition helix undergoes only a slight global translation away from the DNA and a tilt. At a larger level, the displacement of the HTH motif (H1-turn-H2) is accompanied by large conformational changes in the side-chain residues participating in the hydrogen-bond array with the DNA bases (especially the residues Tyr7 and Tyr17).

In the O8 complex, the protein chain including the first three helices and a hydrophobic core, which is expected to present a stable tertiary structure, is located further from DNA than in the G8 complex; therefore, it behaves more like a free chain with the intramolecular interactions prevailing over the intermolecular ones. This explains the decreased flexibility of the protein in the O8 complex. Moreover, as the protein reorganises itself large conformation dispersion of the external residue side chains occurs. Consequently the hydrogen bonds of these residues with the DNA bases are entirely disrupted.

Thus, the comparative flexibility study reinforces the molecular mechanics one: the O8 replacement slightly affects the DNA–protein interaction.

One of the striking points revealed by this study is the extension of the conformational modifications along both the DNA sequence (Fig. 4) and the protein sequence from the A chain to the B chain (Fig. 5). The changes induced by the base replacement in the zone G6T7(**G/O**)8A9 affect not only locally the H2 helix but are spread over the whole B chain as far as the H4 helix. They are then transmitted to the A chain via strong H4–H4 hydrophobic interactions (involving the residues Val52 and Leu56 of the A and B chains), both protein chains acting in a concerted way as a "driving belt" (Fig. 8). Then, the changes are transmitted to the H2 helix of the A chain and thus to the symmetric GTGA zone.

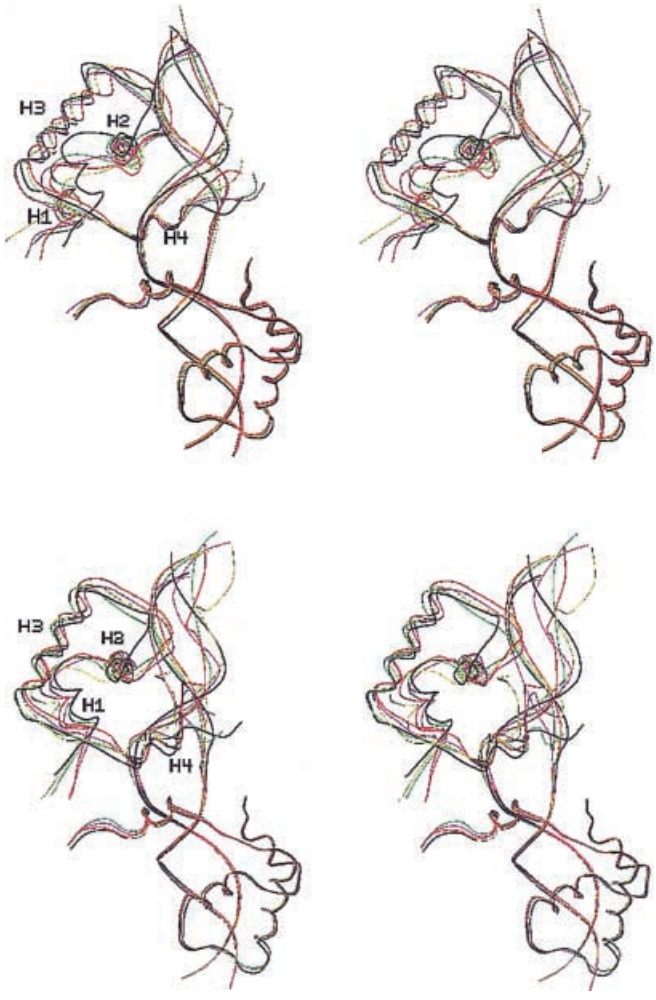

Fig. 7. Stereoview of backbone superposition for the D/G8 (top) and D/O8 (bottom) structures obtained from the simulated annealing protocol

4 Concluding remarks

One can conclude that one or several modified bases 8-oxoG located in the operator sequence only slightly weaken the interactions between the *lac* operator and the *lac* repressor or modify the structure of the *lac* operator–*lac* repressor complex. The most noticeable effects are a 13% decrease in the interaction energy and a 14% reduction in the number of intermolecular hydrogen bonds, all other effects being much weaker. Although they show a tendency for destabilisation, such minor

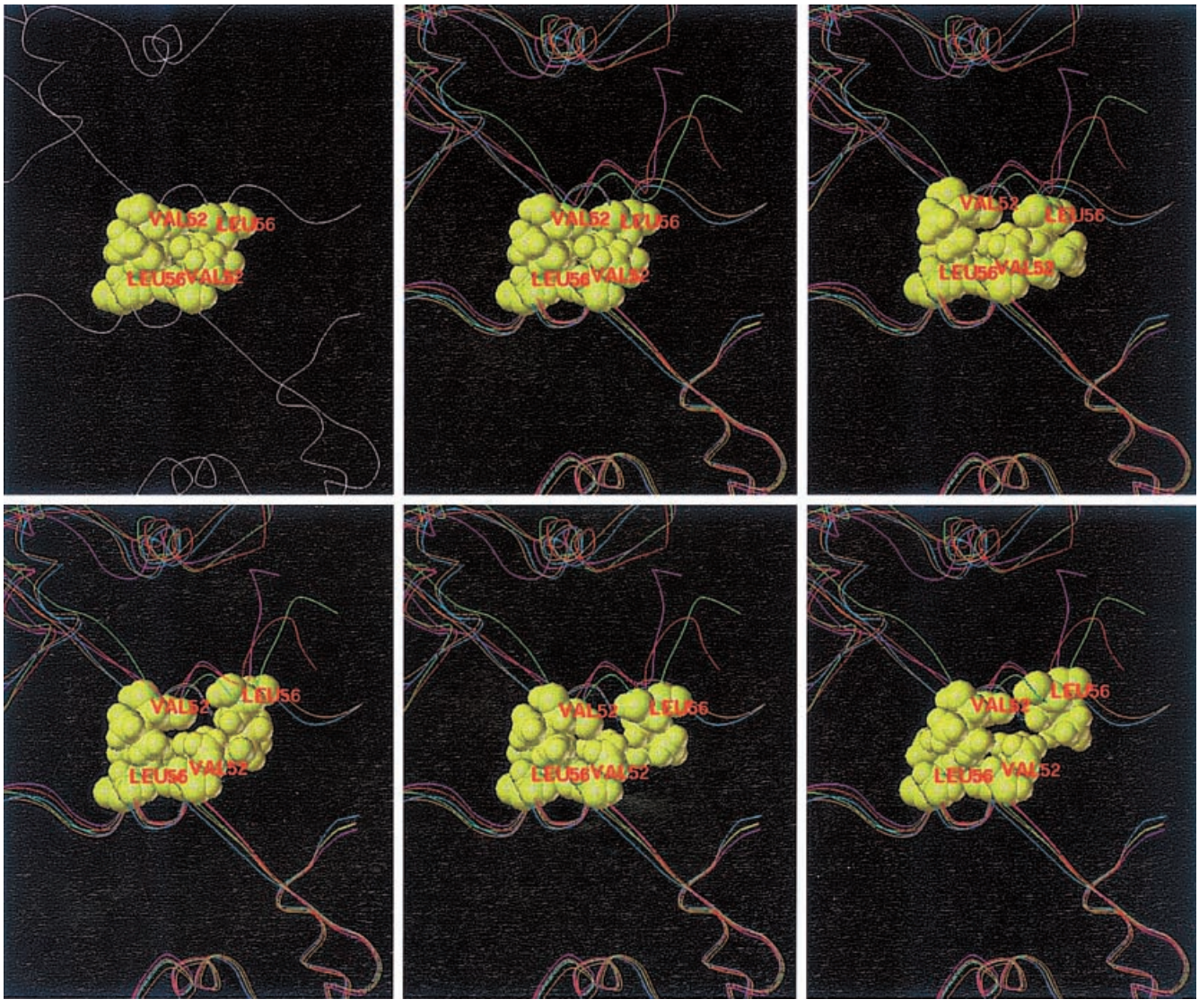

Fig. 8. Persistence of the H4–H4 hydrophobic interaction. *Top left*: G8 reference complex. *Top center*: minimised O8 complex. *Top right* and the *three bottom views*: simulated annealing structures. The snapshots are centered on the antiparallel H4 helices of the chains A (*up*) and B (*down*). The DNA is not displayed

effects are insufficient to account alone for the experimentally observed radiation-induced destruction of the specific DNA–protein complex.

This conclusion is consistent with that of an experimental study in which synthetic modified oligonucleotides (with oxoG instead of G at unique positions) were used. Depending on the replacement position only a 0–30% decrease in the binding of the transcription factors Sp1 to the modified cognate sequence was observed [7].

The molecular modelling approach has to be applied to all other DNA damages (strand breaks, abasic sites and sugar modifications) as well as to combinations of different types of lesions. Moreover, the energetic and structural consequences of possible protein damages (chain breaks and amino acid modifications [17]) also have to be investigated. Such a molecular modelling-based screening can allow the identification of the most critical lesions and thus the reduction of the number of experiments with synthetic modified oligonucleotides and peptides.

References

1. Von Sonntag C (1987) Chemical basis of radiation biology. Taylor and Francis, London
2. Ward J (1988) Prog Nucleic Acid Res Mol Biol 35: 95
3. Goodhead D (1994) Int J Radiat Biol 61: 7
4. Kiefer J (1990) Biological radiation effects. Springer, Berlin Heidelberg New York
5. Wood M, Dizdaroglu M, Gajewski E, Essigmann (1990) Biochemistry 29: 7024
6. Floyd R (1990) Carcinogenesis 11: 1447
7. Ramon O, Sauvaigo S, Gasparutto D, Faure P, Favier A, Cadet J (1999) Free Rad Res 31: 217
8. Plum G, Grollman A, Johnson F, Breslauer K (1995) Biochemistry 34: 16148
9. Barone F, Cellai L, Giordano C, Matzeu M, Mazzei F, Pedone F (2000) Eur Biophys J 28: 621

10. Ninaber A, Goodfellow J (1998) J Biomol Struct Dyn 16: 651
11. Barbier B, Charlier M, Culard F, Durand M, Maurizot J-C, Schnarr M (1983) In: Helene C (ed) Structure, dynamics, interactions and evolution of biological macromolecules. Reidel, Dordrecht, p 141
12. Lewis M, Chang G, Horton N, Kercher M, Pace H, Schumacher M, Brennan R, Lu P (1996) Science 271: 1247
13. Spronk C, Bonvin A, Radha P, Melacini G, Boelens R, Kaptein R (1999) Structure 7: 1483
14. Lavery R, Sklenar H (1986) J Biomol Struct Dyn 6: 63
15. Neidle S (1982) FEBS Lett 298: 97
16. Packer M, Dauncey M, Hunter C (2000) J Mol Biol 295: 85
17. Weik M, Ravelli R, Kryger G, McSweeney, Raves M, Harel M, Gros P, Silman I, Kroon J, Sussman J (2000) Proc Natl Acad Sci USA 97: 623